Minimally invasive determination of mRNA concentration in single living bacteria

Călin C. Guet, Luke Bruneaux, Taejin L. Min, Dan Siegal-Gaskins, Israel Figueroa, Thierry Emonet and Philippe Cluzel*

The James Franck Institute, Institute for Biophysical Dynamics, Department of Physics, The University of Chicago, 929 E 57th St, Chicago, IL 60637, USA

ABSTRACT

Fluorescence correlation spectroscopy (FCS) has permitted the characterization of high concentrations of noncoding RNAs in a single living bacterium. Here, we extend the use of FCS to low concentrations of coding RNAs in single living cells. We genetically fuse a red fluorescent protein (RFP) gene and two binding sites for an RNA-binding protein, whose translated product is the RFP protein alone. Using this construct, we determine in single cells both the absolute [mRNA] concentration and the associated [RFP] expressed from an inducible plasmid. We find that the FCS method allows us to reliably monitor in real-time [mRNA] down to ~40 nM (i.e. approximately two transcripts per volume of detection). To validate these measurements, we show that [mRNA] is proportional to the associated expression of the RFP protein. This FCS-based technique establishes a framework for minimally invasive measurements of mRNA concentration in individual living bacteria.

INTRODUCTION

A fundamental goal of biology is to correlate cellular processes with molecular events in living cells. Over several decades, fluorescence correlation spectroscopy (FCS) (1–3) has been used to monitor concentration and kinetics of biomolecules *in vitro* but it has been only recently applied to living cells. This technique is extremely quantitative because it is self-calibrated and can potentially provide absolute concentration and diffusion times of fluorescent molecules in living cells. For example, FCS was used to characterize the movement of lipid rafts in cell membranes (4), the concentration of signaling proteins in bacteria (5), the presence of active transport in plant cells (6), the change in the viscosity of the nuclear environment

as a function of the cell cycle (7) and the mobility of the highly dynamic Min proteins in bacteria (8). However, only very recently FCS has been used to determine *in vivo* the concentration of nucleic acids such as RNA (9,10).

FCS can detect a wide range of concentrations, from few molecules to 10^3 molecules per detection volume (11). FCS relies on fluctuation analysis of the number of fluorescent molecules diffusing through a small (submicron) detection volume. A small number of molecules will result in large fluctuations of the fluorescent signal, whereas a large number of molecules will decrease the variance of the associated signal relative to its mean (12). The relative fluctuations to the mean of the fluorescence signal are directly related to the absolute number of molecules present in the detection volume. A single FCS measurement provides the absolute concentration and the size of the diffusing fluorescent molecules in a non-invasive way. The submicron size of the FCS detection volume makes the method especially suited for single living cell studies. In principle, any diffusible protein can be fused to a fluorescent marker such as GFP, whose concentration can be quantified with FCS in a living single cell. Recently, we used a FCS-based assay to measure high concentrations of a non-coding RNA in single living bacteria (9). However, it is not known if this method is applicable to the detection of active mRNA transcripts in living cells. In addition, these previous studies (9,13) have not explored *in vivo* the low concentration regime of detection of RNA.

In Le *et al*. (9), a fusion of an RNA-binding protein, MS2-GFP, binds specifically to a tandem of 23-nt RNA-binding sites (14). When MS2-GFP molecules are free, they diffuse fast through the volume of detection with a typical time of ~1 ms. When the MS2-GFP molecules bind to the tandem of RNA-binding sites, the fluorescent molecules diffuse slower, revealing the presence of the specific RNA molecules. The pre-expression of MS2-GFP allows us to monitor variations in RNA concentration on the fly without being limited by the long maturation

*To whom correspondence should be addressed. Tel: 773-834-9096; Email: cluzel@uchicago.edu
Present addresses:
Taejin L. Min, Department of Physics, 1110 West Green, University of Illinois at Urbana Champaign Urbana, IL 61801, USA
Thierry Emonet, MCDB, Yale University New Haven, CT 06510, USA

time of GFP. Additionally, the fusion of a ribosomal binding site to the tandem of RNA-binding sites drastically increases the sensitivity of detection by causing the RNA/MS2-GFP/ribosome complex to diffuse 30-fold slower ($\sim$30 ms) than free MS2-GFP. Due to the strong binding of MS2-GFP to its RNA-binding sites (15), effectively all target RNA molecules in the cell are labeled at all times. Using this molecular labeling scheme, FCS has allowed us to measure the relative concentrations of slow diffusing RNA/MS2-GFP complexes and fast diffusing MS2-GFP proteins. In our previous study (9), a single ribosome binds to each non-coding RNA transcript. MS2-GFP, RNA and the bound ribosome form a well-defined molecular system that unequivocally determines the diffusion of this complex. In this report, we extend the use of the FCS technique from non-coding RNA detection to that of mRNA in single living bacteria of *Escherichia coli*. Each mRNA transcript is actively translated in the cell and thus can have more than one bound ribosome at any given time, making the measurement of [mRNA] potentially more challenging. However, we show that our FCS assay is able to reliably measure mRNA levels in single living cells. We demonstrate that the lower limit of [mRNA] detection is a few tens of nanomolar, which corresponds to about two mRNA transcripts per volume of detection. We also measure simultaneously in each cell the concentration of a red fluorescent protein [RFP] expressed from the measured [mRNA]. Finally, we use the independent measurements of [RFP] to validate the accuracy of [mRNA] measured with FCS.

MATERIALS AND METHODS

Strains and plasmids

We use the strain Frag1B, wild-type for the multi-drug efflux pump *acrAB*, and the strain Frag1A, a deletion mutant of the efflux pumps genes *acrAB* (9). We modified the MS2-GFP fusion protein initially developed by Bertrand *et al.* (14) and described in ref. (9). We introduce a five amino acid linker (Ser, Gly, Gly, Gly and Gly) between the C-terminal of the ΔlFG mutant MS2 coat protein (16) and the N-terminal of the GFP coding part of the fusion gene.

Plasmid pZS*12-MS2-GFP. A fusion-PCR reaction using the five amino acid linker as an internal primer produced the MS2-GFP fusion. The *ms2-gfp* fusion gene was cloned between the KpnI and HindIII sites of a pZS*12 vector (17) to produce *pZS*12-MS2-GFP*.

Plasmid pZE31-dsRed-ms2x2. We used plasmid pQE31-DsRed.T3f (a gift from the Glick Lab, The University of Chicago), which carries the gene for a variant of the fast folding DsRed.T3 (18), to PCR amplify the *dsRed* gene and clone it into a pZE21 vector resulting in plasmid pZE21-DsRed. The two ms2-binding sites were PCR amplified from pZE31-ms2 (9) flanked by HindIII restriction sites with the following primers (5′ – ttaagcttgata tcgaattccga and 3′ –aagcttccgctctagaactagtggatcc). This fragment was introduced into the HindIII site of plasmid

pZE21-DsRed, producing plasmid pZE21-DsRed-ms2x2. Subsequently, the kanamycin resistance cassette was replaced with a chloramphenicol resistance cassette from the pZE series of vectors (17), resulting in the plasmid pZE31-DsRed-ms2x2. Electro-competent cells of both Frag1B and Frag1A were transformed with plasmids pZS*12-MS2-GFP and pZE31-DsRed-ms2x2.

Growth conditions

Cells were grown from a single colony overnight for 14 h in Luria Broth (LB) medium, at 30°C and 300 r.p.m., in the presence of IPTG (200 μM) and the antibiotics ampicillin (50 μg/ml) and chloramphenicol (20 μg/ml). Cells were diluted 1:100 into fresh LB medium, and induced with anhydrotetracycline (aTc) at various concentrations. Cells were grown on average for 2.5–3 h, and harvested at an OD of 0.150–0.200. The same overnight culture was used for all different aTc induction levels, by growing distinct cultures. A 0.3 μl drop of cell culture was placed on a glass cover slip then covered with a 3% low melting-point agarose LB gel containing equal concentrations of aTc as the liquid culture. The gel padding did not contain any antibiotics or IPTG. The sample was sealed within the cavity of an aluminum slide. The prepared sample was then placed on a heated microscope stage at 30°C for measurements. For the kinetic experiments (Figure 4), cells were grown in liquid as described above, however without the inducer aTc. Cells were identically prepared for FCS and we induced them at time $t = 0$ by using a gel padding containing 10 ng/ml aTc.

Single cell measurements

FCS measurements were performed on individual cells within the first hour after harvest. On average 70–80 different cells were measured for each inducer concentration. The fluorescence signal was acquired over a 3 s interval. For the kinetic experiments (Figure 4), we chose individual cells on which we performed FCS measurements every 10–12 min for up to 3 h. When cells were divided we performed measurements on both daughter cells and their descendants.

FCS apparatus

A collimated laser beam (Sapphire 488 nm, 20 mW, Coherent, Santa Clara, CA, USA) is expanded 10-fold via an achromatic diverging lens ($f_2 = 25$ mm) and a converging lens ($f_1 = 250$ mm) to a diameter of $\sim$8 mm. Two neutral density filters (OD = 1 and OD = 3, NE10A and NE30A, Thor Labs, Newton, NJ, USA) attenuate the expanded laser beam before it enters the microscope (OlympusX71, Melville, NY, USA). A dichroic mirror, DM1 in Figure 1, reflects the incoming laser beam, (492dclp Chroma Technologies, Rockingham, VT, USA) and is focused with a $100 \times$ microscope objective lens (NA = 1.3) to a diffraction limited spot onto a single bacterium. The fluorescence signals from the green and red fluorescent proteins are transmitted by DM1 and rejected by a second dichroic mirror, DM2 in Figure 2, (700 dcxr, Chroma Technologies) outside the microscope. The fluorescence light coming out of the microscope
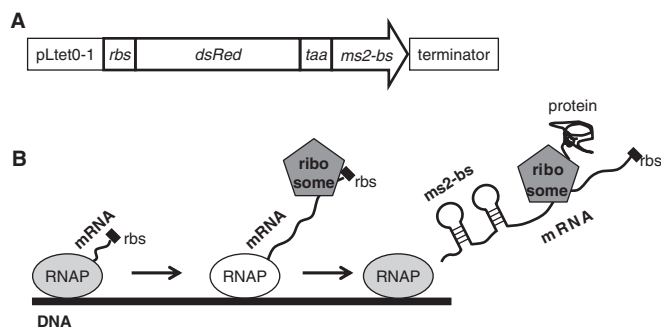
Figure 1. Genetic assay for mRNA/protein measurements in single living cells. (**A**) Transcriptional fusion of the RFP DsRed coding region fused to two ms2-binding sites. The *dsRed-ms2x2* gene was placed under the control of an inducible Tet promoter, pLtetO-1. *rbs*, ribosomal binding site, *taa*, in frame stop codon; *terminator*, transcriptional terminator. (**B**) A molecule of RNA polymerase transcribes the *dsRed-ms2x2* gene. Transcription of the *ms2*-binding sites occurs after the *dsRed* gene. The ribosome binds the nascent mRNA transcript (middle cartoon) and the MS2-GFP proteins binds the mRNA transcript once the *ms2*-binding sites are fully transcribed. This genetic design guarantees that our FCS detection method only measures mRNA transcripts that are free to diffuse and that are not in complex with the RNA polymerase and the DNA.
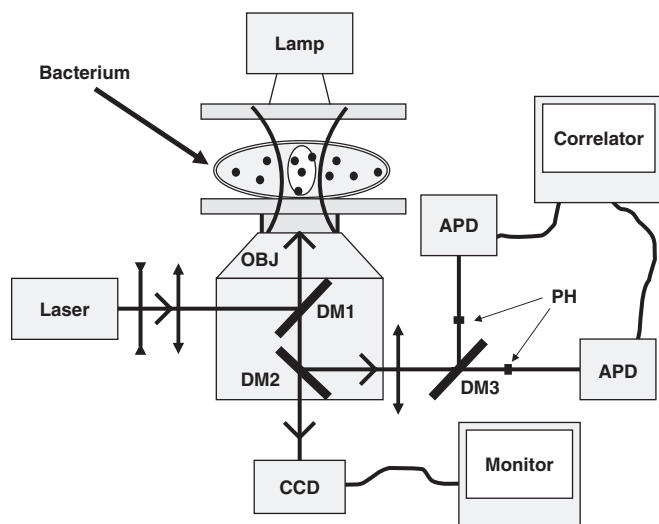

Figure 2. Experimental FCS setup. A 488 nm laser beam is expanded using a divergent and a convergent lens. The expanded beam feeds a Olympus X71 microscope and a dichroic mirror (DM1) reflects the laser blue light on the bacterium. The emitted green and red light from the fluorescent proteins expressed in the bacterium are transmitted through the dichroic mirror (DM1) and are reflected by a second dichroic mirror (DM2). A third dichroic mirror (DM3) splits the fluorescent signal into a green component and a red component. The light is focused with an achromatic convergent lens onto the cores of two optical fibers, which act as pinholes (ph) and feed two avalanche photodiodes (APD) that produce photon counting time series. An ALV correlator connected to a computer records the time series and computes in real-time the associated autocorrelation functions. A red light (lamp) illuminates the sample from above, and a CCD camera is connected to a monitor (more details in Materials and methods section).

is then focused using an achromatic convex lens ($f = 250$ mm, ThorLabs). A high-pass filter (RazorEdge LP02-488RU, Semrock) removes residual 488 nm laser light from the fluorescent signal. The fluorescence light is separated into two components, green and

red, with a third dichroic mirror, DM3 (Figure 2), (575dcxr, Chroma Technologies). A band-pass filter (FF01-520/35, Semrock) selects the green signal and a band-pass filter (FF01-618/50, Semrock) selects the red signal. The cross contribution from the GFP and DsRed fluorescent signal is 2.4% in the green channel and 8.6% in the red channel. Finally, each signal is collected in a confocal geometry using a multimode optical fiber (AFS50/125Y, ThorLabs) whose 50 μm core acts as a pinhole. Photons are detected at the other end of the fiber with a photon counting module (avalanche photodiode spcmaqr-16fc, Perkin Elmer, Vaudreuil, Quebec, Canada). A sub-micrometer positioning system allows us to adjust the *x*, *y*, *z* position of the pinhole, which is critical to FCS measurements. A fast correlator (5000EPP, ALV, Langen, Germany) computes in real-time the autocorrelation function from the fluorescence signal detected by the photon-counting module.

Analysis of FCS measurements

The autocorrelation function of the green fluorescence intensity signal is fitted with the following function:

$$G(t) = \frac{1}{N}\frac{1}{[1+y]^2}\left(\frac{1-y}{(1+t/\zeta_{\text{free}})} + \frac{4y}{(1+t/\zeta_{\text{bound}})}\right)$$

This function models the free and bound MS2-GFP as two species with fast and slow diffusion (19). This model also accounts for the 2-fold increase in brightness per bound species, as every mRNA transcript carries two *ms2*-binding sites, each binding a MS2-GFP homodimer (9). N represents the number of individual fluorescent particles in the observation volume, y is the fraction of MS2-GFP molecules bound to the mRNA–ribosome complex and ζ_{free} and ζ_{bound} represent the diffusion times of free and bound MS2-GFP, respectively. N and y are the fitting parameters. We obtain ζ_{free} by performing FCS measurements on cells carrying only the pZS*12-MS2-GFP plasmid and by fitting the autocorrelation curves with the following function:

$$G(t) = \frac{1}{N}\left(\frac{1}{(1+t/\zeta_{\text{free}})}\right)$$

ζ_{free} is 1.55 ± 0.07 ms in Frag1B cells and 1.59 ± 0.08 ms in Frag1A cells.

A fitting procedure using the two-component function determines the value of ζ_{bound} for each strain (Frag1B and Frag1A) induced with 10 ng/ml aTc. This procedure uses ζ_{bound} as a free parameter to simultaneously minimize the total residual sum of squares for all the autocorrelation functions. We find that ζ_{bound} is 28 ms for Frag1B cells and 29.4 ms for Frag1A cells.

Several factors affect the quality of FCS measurements: excessive bleaching of the GFP molecules and misalignment of the focused laser beam with the cell. A set of selection criteria based on the quality of the autocorrelation curve fit allows us to discard poor-quality FCS measurements. These criteria emerge from the noise analysis of each autocorrelation curve (20,21), as well as a set of empirical observations that relate the number of

fluorescent MS2-GFP measured in the detection volume to the associated mean fluorescence intensity.

Autocorrelation curve noise analysis. At long timescales ($\Delta\tau_j$ longer than 4.5 ms), low-quality autocorrelation data exhibits large deviations from the fit. Several phenomena are responsible for these deviations: poor positioning of the confocal volume on cells, bleaching of the GFP, which artificially introduces a long-time component in the autocorrelation function and large aggregates of fluorescent proteins. The deviations resulting from misalignment occur at time scales larger than ~30 ms (Figure S1). This behavior was readily apparent during data acquisition and we discarded immediately these curves without further analysis. To characterize the effect of bleaching and the presence of poorly diffusing aggregates, we use Fourier analysis of the normalized residuals. We use two parameters: (i) the power spectrum of the normalized residuals at frequency zero, which indicates the presence of a constant component associated with non-diffusing aggregates in the autocorrelation curve and (ii) the variance of the residuals over time scales from 4.5 to 524 ms. We reject curves when the zero-frequency value exceeds 0.03 or the long-time scale residual variance is above 0.2. In Figure S2, we show typical examples of autocorrelation curves that passed or failed this analysis. For the kinetic experiments, the selection values of the two parameters were relaxed by 20% (0.036 and 0.24, respectively).

At short-times scales (dwell times $\Delta\tau_j$ shorter or equal to 256 μs), the autocorrelation function is computed from linearly distributed dwell times $\Delta\tau_j$. Consequently, the variance of the residuals at these time scales should be proportional to $(\Delta\tau_j)^{-1}$. We reject individual autocorrelation curves if the variance at a given time scale deviates from the linear fit by more than 0.4 (Figure S2). For the kinetic experiments, the selection value of the parameter was relaxed by 20% (0.48).

Monomer number and fluorescence intensity. Under working conditions, the total number of MS2-GFP molecules in the detection volume, $N(1 + y)$, is proportional to the measured mean fluorescence intensity. We reject FCS measurements that deviate by >30% from the linear relationship between $N(1 + y)$ and mean fluorescence intensity in the detection volume, as an indication of fluorescent protein aggregation and excessive bleaching.

Bleaching during measurements. Bleaching of MS2-GFP reduces as a function of time the mean fluorescence intensity during signal acquisition. To characterize this decay, we divided the acquisition time (3 s) into 16 intervals. We take the mean of the fluorescence intensity over each interval and fit the 16 means with a line. We rejected measurements that give linear fits with a slope steeper than −6% or +8%.

Determining the number of DsRed molecules. The low quantum efficiency of DsRed sometimes yields a poor signal to noise ratio in our FCS measurements. Nevertheless, we used measurements on cells for which we were able to determine a linear relationship between the number of DsRed molecules and the measured fluorescence intensity (Figure S3). During our measurements, we use this linear relationship to directly infer the number of DsRed molecules and we determine simultaneously [mRNA] using FCS.

Volume of detection of FCS setup

In order to determine the detection volume of the FCS setup, we used fluorescent polystyrene beads of known size (44 nm in diameter, Duke Scientific, Palo Alto, CA, USA). To measure the diffusion coefficient of the beads, we fit the measured autocorrelation function to

$$G(t) = \frac{1}{N}\left(\frac{1}{(1 + 4Dt/\omega^2)}\right)$$

This function describes a 2D translational diffusion process for a fluorescent molecule, where N is the number of diffusing particles in the confocal volume, D is the 2D diffusion constant, t is time and ω is the radius of the detection volume. Using the Stokes–Einstein relationship $D = k_B T/6\pi\eta R$, where k_B is the Boltzman constant, T is temperature in Kelvin (300 K), η is the viscosity of water (1 mPa·s) and R is the radius of the beads (22 nm), we find $D = 10\ \mu m^2/s$. Using $D = \omega^2/4\zeta$, where ω is the radius of the detection volume and ζ the measured diffusion time of the beads (1.01 ms, Figure S4), we determined that $\omega = 0.2\ \mu m$.

Next, we estimate the width of the *E. coli* cells as follows: we image polystyrene beads of known size (diameter = 1.0 μm) together with individual *E. coli* cells and compare the width of the cells to the size of the beads. We find that the average width of the cells is ~0.73 μm. Since the diameter of the detection volume is smaller than the width of the cell, we assume the volume of detection to be a cylinder and compute the volume of detection as: $V_{detection} = \pi\omega^2 h$, where h is the volume height determined by the width of the cell (in this case $h = 0.73\ \mu m$). We find that the volume of detection is thus ~0.09 fl. The presence of one molecule in this volume corresponds to a concentration of ~18.5 nM.

Rate of translation

Based on both mRNA and DsRed concentration measurements we evaluated the mean translation rate per mRNA. We find that the relationship between transcription and translation is linear (Figure 3C): [DsRed] = a[mRNA], with $a = 0.11$ for Frag1B and $a = 0.10$ for Frag1A. Under this steady-state condition, one mRNA transcript corresponds to about 100 DsRed tetramers (~400 monomers of protein). The division time, T, of Frag1B cells growing with 10 ng/ml [aTc] in liquid culture is $T = 42$ min. Since $T = \ln2/\mu$, the resulting growth rate is $\mu = 0.016\ min^{-1}$. The rate of production of DsRed monomers, P, is: $d[P]/dt = k[mRNA] - \mu[P]$ where k is the translation rate per mRNA molecule. At steady state, $k = \mu[P]/[mRNA]$. We find $k = 6.7$ DsRed monomers per mRNA transcript per minute. The *dsRed* gene codes for 220 amino acids, and if we assume on average three ribosomes loaded per mRNA message (22), we find that the average translation
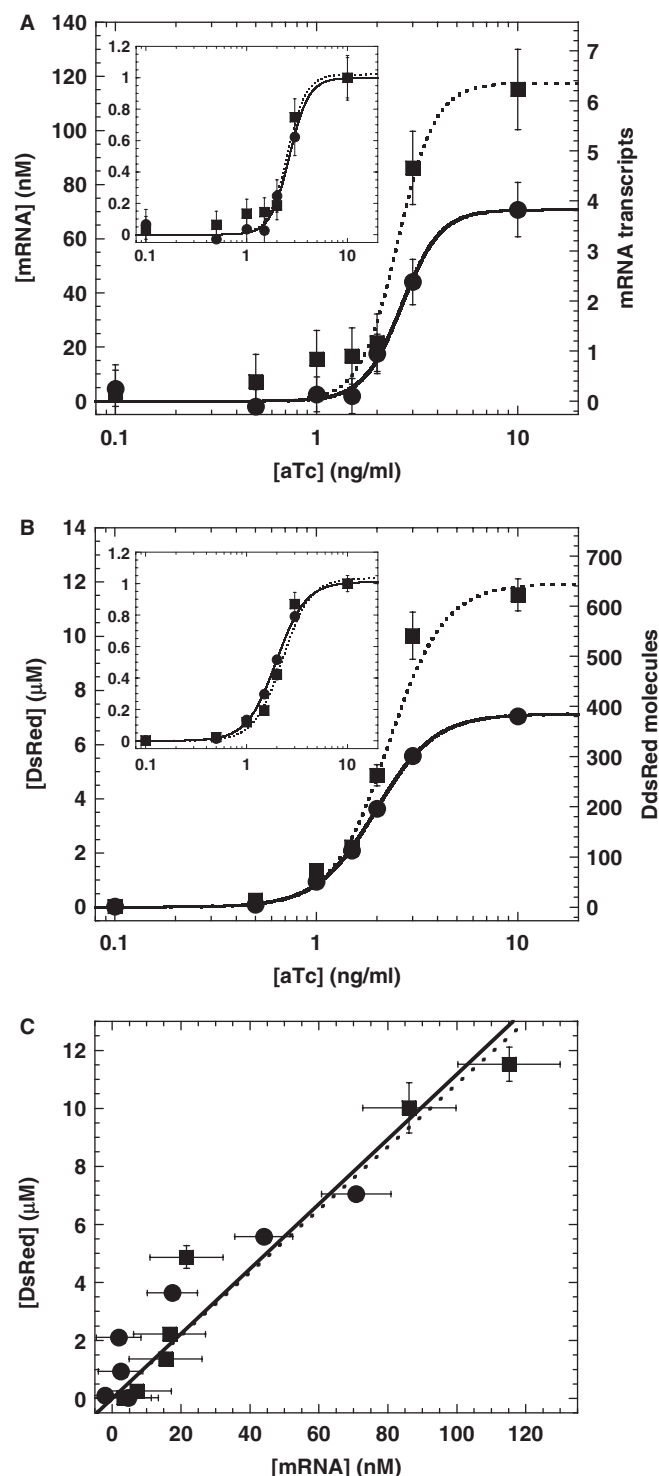
Figure 3. (**A**) A [mRNA] (nM) as a function of inducer concentration. Each data point represents the average mRNA concentration measured across 30–60 individual Frag1B (circles and solid line) and Frag1A (squares and interrupted line) cells. The number of mRNA transcripts present in the detection volume is converted into a concentration (nM). The farthest point on the left of the graph represents [mRNA] measured in the absence of inducer (0 [aTc]). The inset represents a Hill fit of the normalized data with Hill coefficient ∼4.5 ± 1.6 for Frag1B and 4.6 ± 1.5 for Frag1A. Error bars represent the combination of the standard error and the systematic error, the latter is determined from the measured [mRNA] in a cell with no pZE31-DsRed-ms2x2 plasmid. This value was 6 nM for Frag1B and 10 nM for Frag1A and was subtracted from all data points. (**B**) DsRed tetramer concentration (μM) as a function of inducer level. Each point represents the average protein concentrations measured across the same individual cells as in (A). Error bars represent the standard error. The number of DsRed tetramers in the detection volume is converted into concentration (μM) on the left side of the graph. The farthest point on the left of the graph is [DsRed] in the absence of inducer (0 aTc). The inset represents a Hill fit of the normalized data with Hill coefficient of 3 ± 0.2 for Frag1B and 3.1 ± 0.3 for Frag1A. Frag1B, circles and solid line; Frag1A, squares and interrupted line. (**C**) Protein and mRNA concentrations within the detection volume. Frag1B, circles; Frag1A, squares. Linear fit (forced through 0): dashed lines (Frag1B) with R factor of 0.94, continuous line (Frag1A) with R factor of 0.97.
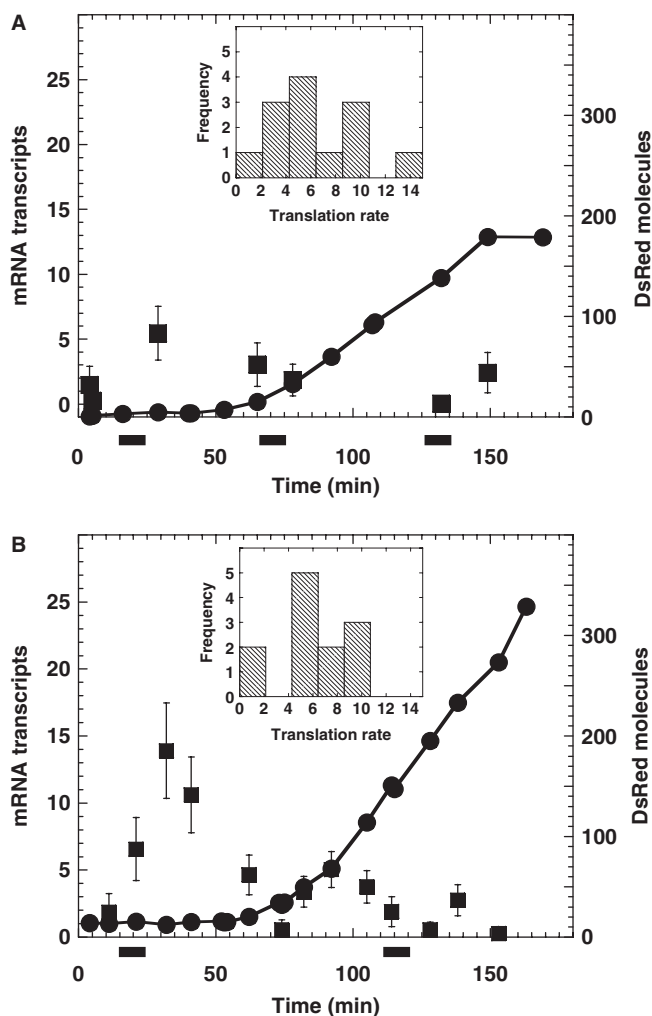
rate for an individual ribosome is about eight amino acids per second. This rate is consistent with the translation rates of previous studies (23,24).

In order to calculate the translation rate per mRNA, $k_{kinetic}$ from kinetic experiments (Figure 4), we use individual measurements of concentration, average division time and volume of the cell. We hypothesize that the cell body grows linearly with time from an initial volume, V_0, to a final volume, $2V_0$, during one division time, T, such as $V(t) = V_0(1 + t/T)$. In each cell, we monitored the concentration of RFP, $[P](t)$, which increases linearly over at least one division time such that $[P](t) = P_0 + bt$ where P_0 and b are the initial concentration and rate of protein synthesis (uncorrected for growth) for a given cell, respectively. Since the total number of RFP molecules in the cell at time t is given by $n(t) = [P](t) V(t)$, the number of molecules produced during a time interval t will be $\Delta n = [P](t) V(t) - P_0 V_0$. We can estimate the translation rate per mRNA transcript per minute for the kinetic experiments during one cell division as:

$$k_{kinetic} = \frac{V_0}{R_{mean}} \left[\frac{P_0}{T} + 2b \right]$$

where R_{mean} is the average number of mRNA transcripts calculated over the corresponding time interval shifted back by 80 min to account for DsRed maturation time. We use $V_0 \approx 1\,\mu m^3$ and $T = 60\,min$ (for cells growing on the gel padding), and the measured values of R_{mean}, P_0 and b.

RESULTS

Genetic assay for mRNA/protein *in vivo* measurements

We construct a synthetic gene to simultaneously measure mRNA and associated protein levels. The gene sequence carries at the level of DNA a coding region for the RFP DsRed followed by a tandem of two *ms2*-binding sites, *ms2x2*, and ends with a transcriptional terminator (Figure 1A). A stop codon in the *dsRed* gene ensures that translation does not proceed beyond the *dsRed* coding region into the noncoding *ms2x2*-binding sites. The resulting synthetic gene, which we call *dsRed-ms2x2*, is very tightly controlled by an inducible TetR regulated promoter (17). The coding region of DsRed is at the 5′ end of the ms2-binding sites. Therefore, the *dsRed* gene is transcribed first and the *ms2x2*-binding sites last (Figure 1B). This order ensures that MS2-GFP molecules bind the mRNA transcript only after the gene has been

Figure 4. Kinetics of transcription and translation in single cells. Individual cells were induced with 10 ng/ml aTc at time $t = 0$. (**A**) Frag1B cells—wildtype for the efflux pumps genes *acrAB*. (**B**) Frag1A cells—*acrAB* deletion mutant. mRNA concentration (squares) and DsRed concentration (circles) were measured with FCS in single cells. Error bars associated with mRNA measurements were determined as in ref. (9). Horizontal bars at the bottom of the graphs indicate cell division events. Insets: distribution of translation rates per mRNA (monomers/mRNA/min) measured in different individual cells. In Frag1B cells, mean mRNA concentration: 3.7 ± 1.3 transcripts; mean rate of DsRed synthesis (not corrected for growth): 10.6 ± 4.7 monomers/min; mean translation rate per mRNA: 6.5 ± 3.4 monomers/mRNA/min. In Frag1A cells, mean mRNA concentration: 6.9 ± 2.7 transcripts; mean rate of DsRed synthesis (not corrected for growth): 15.5 ± 5 monomers/min; mean translation rate per mRNA: 5.9 ± 2.8 monomers/mRNA/min.

fully transcribed, guaranteeing that we detect only fully transcribed mRNA transcripts. MS2-GFP fusion proteins are pre-expressed in the cytoplasm from a low-copy plasmid and are immediately available to bind the mRNA coded by the *dsRed-ms2x2* gene.

Using FCS to monitor mRNA concentration

FCS is a technique sensitive to the diffusion coefficient of fluorescent molecules (2). We can detect *dsRed-ms2x2* mRNA transcripts during translation because the binding

of ribosomes drastically increases the diffusion time of mRNA transcripts bound by MS2-GFP molecules. Using FCS we determine the fraction, y, of bound MS2-GFP molecules, and we infer the number of mRNA transcripts present in the detection volume.

In this inducible Tet promoter system, the average [mRNA] measured across a population of individual cells increases with [aTc] (Figure 3A). We use two different strains, a wild-type (Frag1B) and the *ΔacrAB* null mutant (Frag1A) for multi-drug resistance efflux pumps (25). We find that in both the wild-type and mutant strains, [mRNA] increases with [aTc] in a sigmoidal fashion (Figure 3A). The observed sigmoidal curves are indicative of a cooperative mechanism in the regulation of the transcription process (Hill coefficients ~4). The fact that [mRNA] induction curves for strains Frag1B and Frag1A have sigmoidal curves with similar Hill coefficients, but exhibit different levels of expression further validates our method. The presence or absence of the *acrAB* efflux pumps in these two strains affects the internal aTc concentration; the absence of the *acrAB* efflux pumps in strain Frag1A results in higher levels of mRNA than in Frag1B (~2-fold higher for the highest aTc induction level). However, the difference between the two strains should not affect the cooperative nature of the TetR regulation system, as seen in Figure 3A.

Simultaneous detection of protein concentration by fluorescence intensity levels

As the main validation of our [mRNA] measurements, we monitor the fluorescence intensity from the translated *dsRed* gene. Our inducible genetic system is regulated solely at the transcriptional level and uses TetR as repressor and aTc as inducer. Consequently, if the FCS measurements of [mRNA] are robust, the induction curve of [mRNA] and [DsRed] should exhibit a similar expression profile. As expected, the induction curves of mRNA (Figure 3A) and DsRed (Figure 3B) as a function of [aTc] yield comparable Hill coefficients. Moreover, we also find that the induction curves of [DsRed] in wild-type and mutant cells have similar Hill coefficients of ~3 (Figure 3B, inset). The similarity between the Hill coefficients across strains, mRNA and protein measurements constitutes an additional control for our method. Figure 3C shows the direct relationship between mRNA and protein levels in wild-type Frag1B and mutant Frag1A cells. Both strains display a similar linear relationship between transcription and translation, and the slope allows us to estimate a translation rate of approximately eight amino acids per second. This rate is in agreement with that of the visualization method for mRNA determination (26).

We previously showed that mutant Frag1A cells expressed more proteins than wild-type Frag1B cells (27). However, this effect was observed at much higher levels of the inducer aTc (400 ng/ml) than the levels used in the present study. The 2-fold difference in expression between the two strains observed at the level of mRNA is also present in the levels of [DsRed] in Figure 3B.

Kinetics of transcription and translation in single cells

We demonstrate the ability of FCS to monitor the kinetics of transcription and translation in single cells throughout the growth and divisions of single cells (Figure 4). In these kinetic experiments, we induce the cells at time $t = 0$ with 10 ng/ml aTc and measure as a function of time mRNA transcript numbers (Figure 4A and B). The steady slope of the DsRed concentration allows us to determine an approximation of the translation rate per mRNA for DsRed during induction. We determine the rate for DsRed synthesis over a fixed time interval after exposure to a steady level of the aTc inducer and we also account for cell growth (Figure 4, insets). We approximate the mean value of [mRNA] over the same time interval, however shifted back by 80 min to account for the maturation time of DsRed. We find the same mean translation rate per mRNA for wild-type Frag1B cells (6.5 monomers/mRNA/min) and the efflux pump mutant Frag1A (5.9 monomers/mRNA/min). This translation rate is also similar to the rate found from our steady-state study in Figure 3C (6.7 DsRed monomers/mRNA/min). However, we find that translation rates are widely distributed at the single cell level (Figure 4, insets). This wide distribution may be due to fast variations of [mRNA] that are smoothed out at the level of accumulated DsRed tetramers. Nevertheless, the mean [mRNA] from about a dozen cells in Figure 4, (Frag1B—3.7 transcripts and Frag1A—6.9 transcripts) is comparable to that of Figure 3A for 10 ng/ml aTc.

DISCUSSION

The combination of a genetic fusion and the FCS technique demonstrates that simultaneous detection of mRNA and its associated protein is technically feasible. In this report, we have extended our approach from the detection of noncoding RNA to that of a coding RNA. The detection of mRNAs by FCS is potentially complicated by the heterogeneous distribution of ribosomes per transcript during translation. The distribution of ribosomes in polysomes has been shown to be narrow and specific for each mRNA species (22). In general, the size of the polysome scales with the length of the mRNA and should be about three ribosomes per polysome for a DsRed-sized mRNA (22). To the first approximation, mRNA in solution behaves like an ideal polymer. The associated hydrodynamic radius of a translated transcript (and hence its diffusion time ζ_{bound}) will vary like the square root of the number of bound ribosomes. Since the average number of ribosomes per mRNA is 3 ± 1 ribosomes, the relative variation in time ζ_{bound} will range from $\sqrt{2}$ to $\sqrt{4}$. This interval is too narrow to be resolved with FCS. Therefore, we coarse-grained the underlying complexity of this molecular system by using only one effective diffusion time for the mRNA in complex with ribosomes. This simplification implicitly attributes to the measured fraction y the meaning of an effective translational activity. The validity of this simplification is supported by the similarity of the Hill coefficients of mRNA and protein induction curves. Presently, our ability to detect in real-time protein concentration is limited by the DsRed protein maturation time of about 80 min (18).

There exist alternative imaging-based methods to measure [mRNA] in living cells. Imaging methods are based on two different approaches. The first approach uses large arrays of *ms2*-binding sites as mRNA probes to bind 96 MS2-GFP fluorescent molecules per mRNA molecule (26,28). This imaging method is superior to FCS when mRNA is localized and does not diffuse freely (see section 'Autocorrelation curve noise analysis'), as is often the case in eukaryotes. A large array of labeling molecules allows for great temporal resolution to monitor the synthesis of new transcript one molecule at a time. However, since this technique relies on the detection of discrete fluorescent aggregates per cell, which represent individual mRNA molecules, there is an upper limit on the concentration of mRNA that can be reliably detected. Furthermore, the large size of this *ms2x96* probe can greatly affect the tertiary structure, degradation and diffusion characteristics of the labeled mRNAs. The presence of very large MS2-GFP aggregates bound to active mRNA potentially restricts the access of ribosomes to the transcript, and lower the steady-state translational rate by 4-fold in ref. (26) compared to our study. A second, more recent state of the art imaging approach employs complementation of split GFP, which is mediated by the presence of a small mRNA probes (29,30). This latter imaging technique is much less invasive and also permits the detection of high [mRNA]. In contrast with the first imaging technique that gives precise number of mRNA transcripts, the data is given in relative unit of fluorescence. Finally, the GFP complementation method has limited temporal resolution due to the maturation time of the split GFP.

Alternatively, FCS-based methods for RNA detection in bacteria have two main characteristics. First, FCS works for both low concentrations (nM) of RNA as we showed here as well as high concentrations (μM) of RNA as we have shown previously in ref. (9). Second, FCS is a minimally invasive detection method. In principle, the small *ms2x2* tag can be cloned at the 3′ end of any bacterial gene, which now makes single cell transcriptome FCS analysis technically attainable (31). More generally, the ability to determine levels of mRNA over a wide range of concentrations in real-time should be useful for synthetic biology where the use of high-copy plasmids can lead to high intracellular [mRNA] levels. It should also be potentially useful in phage biology where low and very high [mRNA] are present during lytic and lysogenic growth. Together, FCS and imaging-based methods offer a broad range of solutions for the detection of any type of RNA species, whether present in small or large numbers, localized or freely diffusing.

SUPPLEMENTARY DATA

Supplementary Data are available at NAR Online.

ACKNOWLEDGEMENTS

Conflict of interest statement. None declared.

REFERENCES

1. Magde,D., Elson,E.L. and Webb,W.W. (1974) Fluorescence correlation spectroscopy. 2. Experimental realization. *Biopolymers*, **13**, 29–61.
2. Magde,D., Webb,W.W. and Elson,E. (1972) Thermodynamic fluctuations in a reacting system–measurement by fluorescence correlation spectroscopy. *Phys. Rev. Lett.*, **29**, 705–708.
3. Elson,E.L. and Magde,D. (1974) Fluorescence correlation spectroscopy. 1. Conceptual basis and theory. *Biopolymers*, **13**, 1–27.
4. Bacia,K., Scherfeld,D., Kahya,N. and Schwille,P. (2004) Fluorescence correlation spectroscopy relates rafts in model and native membranes. *Biophys. J.*, **87**, 1034–1043.
5. Cluzel,P., Surette,M. and Leibler,S. (2000) An ultrasensitive bacterial motor revealed by monitoring signaling proteins in single cells. *Science*, **287**, 1652–1655.
6. Kohler,R.H., Schwille,P., Webb,W.W. and Hanson,M.R. (2000) Active protein transport through plastid tubules: velocity quantified by fluorescence correlation spectroscopy. *J. Cell. Sci.*, **113**, 3921–3930.
7. Wachsmuth,M., Waldeck,W. and Langowski,J. (2000) Anomalous diffusion of fluorescent probes inside living cell nuclei investigated by spatially-resolved fluorescence correlation spectroscopy. *J. Mol. Biol.*, **298**, 677–689.
8. Meacci,G., Ries,J., Fischer-Friedrich,E., Kahya,N., Schwille,P. and Kruse,K. (2006) Mobility of Min-proteins in Escherichia coli measured by fluorescence correlation spectroscopy. *Phys. Biol.*, **3**, 255–263.
9. Le,T.T., Harlepp,S., Guet,C.C., Dittmar,K., Emonet,T., Pan,T. and Cluzel,P. (2005) Real-time RNA profiling within a single bacterium. *Proc. Natl Acad. Sci. USA*, **102**, 9160–9164.
10. Nomura,Y., Nakamura,T., Feng,Z. and Kinjo,M. (2007) Direct quantification of gene expression using fluorescence correlation spectroscopy. *Curr. Pharm. Biotechnol.*, **8**, 286–290.
11. Kim,S.A., Heinze,K.G. and Schwille,P. (2007) Fluorescence correlation spectroscopy in living cells. *Nat. Methods*, **4**, 963–973.
12. Hess,S.T., Huang,S.H., Heikal,A.A. and Webb,W.W. (2002) Biological and chemical applications of fluorescence correlation spectroscopy: a review. *Biochemistry*, **41**, 697–705.
13. Le,T.T., Emonet,T., Harlepp,S., Guet,C.C. and Cluzel,P. (2006) Dynamical determinants of drug-inducible gene expression in a single bacterium. *Biophys. J.*, **90**, 3315–3321.
14. Bertrand,E., Chartrand,P., Schaefer,M., Shenoy,S.M., Singer,R.H. and Long,R.M. (1998) Localization of ASH1 mRNA particles in living yeast. *Mol. Cell*, **2**, 437–445.
15. Johansson,H.E., Dertinger,D., LeCuyer,K.A., Behlen,L.S., Greef,C.H. and Uhlenbeck,O.C. (1998) A thermodynamic analysis of the sequence-specific binding of RNA by bacteriophage MS2 coat protein. *Proc. Natl Acad. Sci. USA*, **95**, 9244–9249.
16. Peabody,D.S. and Ely,K.R. (1992) Control of translational repression by protein - protein interactions. *Nucleic Acids Res.*, **20**, 1649–1655.
17. Lutz,R. and Bujard,H. (1997) Independent and tight regulation of transcriptional units in Escherichia coli via the LacR/O, the TetR/O and AraC/I-1-I-2 regulatory elements. *Nucleic Acids Res.*, **25**, 1203–1210.
18. Bevis,B.J. and Glick,B.S. (2002) Rapidly maturing variants of the Discosoma red fluorescent protein (DsRed). *Nat. Biotechnol.*, **20**, 83–87.
19. Krichevsky,O. and Bonnet,G. (2002) Fluorescence correlation spectroscopy: the technique and its applications. *Reports Progress Phys.*, **65**, 251–297.
20. Wohland,T., Rigler,R. and Vogel,H. (2001) The standard deviation in fluorescence correlation spectroscopy. *Biophys. J.*, **80**, 2987–2999.
21. Saffarian,S. and Elson,E.L. (2003) Statistical analysis of fluorescence correlation spectroscopy: the standard deviation and bias. *Biophys. J.*, **84**, 2030–2042.
22. Arava,Y., Wang,Y.L., Storey,J.D., Liu,C.L., Brown,P.O. and Herschlag,D. (2003) Genome-wide analysis of mRNA translation profiles in Saccharomyces cerevisiae. *Proc. Natl Acad. Sci. USA*, **100**, 3889–3894.
23. Pedersen,S. (1984) Escherichia-coli ribosomes translate invivo with variable-rate. *EMBO J.*, **3**, 2895–2898.
24. Talkad,V., Schneider,E. and Kennell,D. (1976) Evidence for variable rates of ribosome movement in Escherichia-coli. *J. Mol. Biol.*, **104**, 299–303.
25. Li,X.Z. and Nikaido,H. (2004) Efflux-mediated drug resistance in bacteria. *Drugs*, **64**, 159–204.
26. Golding,I., Paulsson,J., Zawilski,S.M. and Cox,E.C. (2005) Real-time kinetics of gene activity in individual bacteria. *Cell*, **123**, 1025–1036.
27. Le,T.T., Guet,O.C. and Cluzel,P. (2006) Protein expression enhancement in efflux-deleted mutant bacteria. *Protein Exp. Purif.*, **48**, 28–31.
28. Golding,I. and Cox,E.C. (2004) RNA dynamics in live Escherichia coli cells. *Proc. Natl Acad. Sci. USA*, **101**, 11310–11315.
29. Valencia-Burton,M., McCullough,R.M., Cantor,C.R. and Broude,N.E. (2007) RNA visualization in live bacterial cells using fluorescent protein complementation. *Nat. Methods*, **4**, 421–427.
30. Ozawa,T., Natori,Y., Sato,M. and Umezawa,Y. (2007) Imaging dynamics of endogenous mitochondrial RNA in single living cells. *Nat. Methods*, **4**, 413–419.
31. Ruan,Y.J., Le Ber,P., Ng,H.H. and Liu,E.T. (2004) Interrogating the transcriptome. *Trends Biotechnol.*, **22**, 23–30.